Georg-August-Universität Göttingen

Fast numerical solution of the electromagnetic medium scattering problem and applications to the inverse problem

Thorsten Hohage

Preprint Nr. 2005-34

Fast numerical solution of the electromagnetic medium scattering problem and applications to the inverse problem

Thorsten Hohage

Inst. für Numerische und Angewandte Mathematik, Lotzestr. 16-18, 37083 Göttingen, Germany, `hohage@math.uni-goettingen.de`

Abstract

We propose a method for computing the scattering of a time-harmonic electromagnetic wave in a medium with a locally perturbed refractive index. We prove that it converges of arbitrarily high order depending on the smoothness of the refractive index and that the time complexity is $O(N^3 \log(N))$. As an application we solve the corresponding inverse problem using a preconditioned Newton method and discuss how to compute the Fréchet derivative of the solution operator and its adjoint by the proposed method. The performance of both the forward and the inverse solver is illustrated in a number of numerical experiments.

Key words: inverse scattering, iteratively regularized Gauß-Newton method, regularization, time-harmonic Maxwell equations, electromagnetic medium scattering problem
PACS: 65N12, 78M25, 65N21, 65N55

1 Introduction

The scattering of electromagnetic waves in a medium with a locally perturbed refractive index is a fundamental problem which arises in medical imaging, scanning near-field microscopy, detection of buried objects, and geophysical explorations. We derive an extension of Vainikko's fast solver for the acoustic Lippmann-Schwinger equation ([1]) to electromagnetic problems. The proposed method is easy to implement, it converges of arbitrarily high order for smooth refractive indices, and its total complexity is of order $O(N^3 \ln N)$ where N is the number of degrees of freedom in each space dimension. Therefore, it is an attractive alternative to the finite element method. As opposed to

FEM, no transparent boundary condition is needed since the radiation condition is incorporated in a natural way through an integral formulation of the forward problem. As a disadvantage of our method, we point out that we do not know how to handle refractive indices with jumps so far. For acoustic problems Vainikko has shown convergence of order $O(N^{-2} \ln N)$ in this case, but due to the lack of regularity, this result cannot be carried over to electromagnetic problems in a straightforward way.

Often the inverse problem to reconstruct the refractive index of a medium from noisy measurements of the scattered field is more important in applications than the forward problem. We also discuss the use of the proposed forward solver in iterative regularization methods and show how to implement the Fréchet derivative of the solution operator and its adjoint needed in such schemes.

Our aim is to solve the inverse problem for single–frequency data in the regime of wave numbers in the resonance region and refractive indices of a size where the problem is both strongly nonlinear and severely ill-posed. To this end we use a preconditioned Newton method as suggested in [2]. This method is well-suited for large-scale nonlinear, exponentially ill-posed problems since it yields accurate reconstructions and significantly reduces the number of forward problem solutions compared to other regularization methods. We discuss the implementation of this method for the inverse electromagnetic medium scattering problem and present numerical results.

Let us review some methods which have been proposed in the literature for the full reconstruction of the refractive index. Natterer, Vögeler & Wübbeling [3,4] have developed an algorithm for the solution of the inverse problem in the case of large wave numbers. They solve the forward problem approximately by a marching scheme in space and the inverse problem by Kaczmarz's algorithm. Their approach is restricted to the important regime of large wave numbers where the large-scale structure of the refractive index can be reconstructed in a stable way. Bao & Li [5] have proposed a method for multi-frequency data where one iteration step is performed for each frequency starting with the lowest one (see also Chen [6]). This reduces the danger of being trapped in a local minimum. To identify the support of the perturbation of the refractive index, Haddar & Monk [7] used a linear sampling method and Kirsch [8] investigated a factorization method. Several researchers have considered the linearized problem (see [9] and references therein). Kleinman & van den Berg have proposed to formulate the inverse problem as an optimization problem both in the refractive index (or its perturbation) and the total electric field (see [10] and references therein). The usefulness of this approach for three-dimensional electromagnetic inversions is limited by extremely large memory requirements as the total fields for all incident waves need to be stored.

The plan of this paper is as follows: After giving a precise definition of the forward problem and its equivalent formulation as the Lippmann-Schwinger integral equation in the following section, we describe our forward solver in section 3 and provide an error analysis of this method. Section 4 is devoted to the numerical solution of the discrete system by multi-grid methods and includes a convergence and complexity analysis. Numerical experiments on the performance of the forward solver are presented in section 5. In section 6 we discuss the implementation of the Fréchet derivative of the solution operator and its adjoint. Finally, in section 7 we introduce a preconditioned Newton method for the solution of the inverse problem and present numerical results.

2 Forward scattering problem

problem formulation. We consider the propagation of time-harmonic electromagnetic waves in an inhomogeneous, non-magnetic, isotropic medium without free charges. Let the time dependence of the electric field $\tilde{\mathbf{E}}$ be described by $\tilde{\mathbf{E}}(\mathbf{x}, t) = \Re\left(\mathbf{E}(\mathbf{x})e^{-i\omega t}\right)$ where $\omega > 0$ is the angular frequency. Moreover, let $\epsilon(\mathbf{x}) > 0$ denote the electric permittivity of the medium, $\sigma(\mathbf{x})$ the electric conductivity, and μ_0 the magnetic permeability, which is assumed to be constant. We further assume that $\epsilon(\mathbf{x}) = \epsilon_0$ and $\sigma(\mathbf{x}) = 0$ for $|\mathbf{x}| \geq \rho$, i.e. the inhomogeneity of the medium is supported in the ball $B_\rho := \{\mathbf{x} \in \mathbb{R}^3 : |\mathbf{x}| < \rho\}$ of radius $\rho > 0$. Then the vector field $\mathbf{E} : \mathbb{R}^3 \to \mathbb{C}^3$ satisfies the differential equation

$$\operatorname{curl}\operatorname{curl}\mathbf{E} - \kappa^2(1 - a(\mathbf{x}))\mathbf{E} = 0 \qquad \text{in } \mathbb{R}^3 \tag{1}$$

where $\kappa = \omega\sqrt{\epsilon_0\mu_0}$ is the wave number and

$$1 - a(\mathbf{x}) = n(\mathbf{x}) = \frac{1}{\epsilon_0}\left(\epsilon(\mathbf{x}) + i\frac{\sigma(\mathbf{x})}{\omega}\right), \qquad \mathbf{x} \in \mathbb{R}^3$$

is the refractive index of the medium. We assume that $n \in C^{1,\alpha}(\mathbb{R}^3)$. Note that $\operatorname{supp} a \subset B_\rho$.

The forward scattering problem is the following: Given an incident field $\mathbf{E}^i$ which satisfies the homogeneous Maxwell equations

$$\operatorname{curl}\operatorname{curl}\mathbf{E}^i - \kappa^2\mathbf{E}^i = 0 \qquad \text{in } \mathbb{R}^3, \tag{2}$$

find a scattered fields $\mathbf{E}^s \in C^2(\mathbb{R}^3, \mathbb{C}^3)$ such that the total field $\mathbf{E} = \mathbf{E}^i + \mathbf{E}^s$ solves the Maxwell equations (1), and the scattered field satisfies the *Silver-Müller radiation condition*

$$\lim_{|\mathbf{x}|\to\infty}\left(\operatorname{curl}\mathbf{E}^s(\mathbf{x}) \times \mathbf{x} - i\kappa|\mathbf{x}|\,\mathbf{E}^s(\mathbf{x})\right) = 0 \tag{3}$$

uniformly for all directions $\hat{\mathbf{x}} = \mathbf{x}/|\mathbf{x}| \in S^2$.

electromagnetic Lippmann-Schwinger equation. Our numerical method is based on an equivalent formulation of the forward problem as an integral equation. For proofs and further information we refer to [11]. Let

$$\Phi(\mathbf{x}) := \frac{e^{i\kappa|\mathbf{x}|}}{4\pi|\mathbf{x}|}, \qquad \mathbf{x} \in \mathbb{R}^3 \backslash \{0\}$$

denote the fundamental solution to the Helmholtz equation. If $\mathbf{E} \in C^2(\mathbb{R}^3, \mathbb{C}^3)$ is a solution to the direct scattering problem (1)-(3), then it satisfies the integral equation

$$\mathbf{E}(\mathbf{x}) + \kappa^2 \int_{B_\rho} \Phi(\mathbf{x} - \mathbf{y}) a(\mathbf{y}) \mathbf{E}(\mathbf{y}) \, \mathrm{d}\mathbf{y} \tag{4}$$

$$+ \mathbf{grad} \int_{B_\rho} \Phi(\mathbf{x} - \mathbf{y}) \frac{\mathbf{grad}\, a(\mathbf{y})}{1 - a(\mathbf{y})} \cdot \mathbf{E}(\mathbf{y}) \, \mathrm{d}\mathbf{y} = \mathbf{E}^i(\mathbf{x}), \quad \mathbf{x} \in \mathbb{R}^3,$$

which is the analog to the acoustic Lippmann-Schwinger equation. Vice versa, if $\mathbf{E} \in C(\mathbb{R}^3, \mathbb{C}^3)$ is a solution to (4), then $\mathbf{E} \in C^2(\mathbb{R}^3, \mathbb{C}^3)$, and $\mathbf{E}$ solves the direct scattering problem (1)-(3). Note that if $\mathbf{E}$ is given on B_ρ, then it is known everywhere since we can solve (4) for $\mathbf{E}(\mathbf{x})$. It follows from the mapping properties of the volume potential that the operator on the left hand side of (4) is of the form "identity + compact". Hence, by Riesz theory and the uniqueness of the forward problem (cf. [11]), eq. (4) has a unique solution $\mathbf{E} \in (L^2(B_\rho))^3$.

far field patterns. It can be shown that a solution to (4) has the asymptotic behavior

$$\mathbf{E}^s(\mathbf{x}) = \frac{e^{i\kappa|\mathbf{x}|}}{|\mathbf{x}|} \left(\mathbf{E}^\infty(\hat{\mathbf{x}}) + \mathcal{O}\left(\frac{1}{|\mathbf{x}|}\right) \right).$$

$\mathbf{E}^\infty$ is called the far-field pattern of $\mathbf{E}^s$ and satisfies $\hat{\mathbf{x}} \cdot \mathbf{E}^\infty(\hat{\mathbf{x}}) = 0$ for all $\hat{\mathbf{x}} \in S^2$, i.e. it is a tangential vector field on the unit sphere. From (4) we obtain the formula

$$\mathbf{E}^\infty(\hat{\mathbf{x}}) = -\kappa^2 \int_{B_\rho} \frac{e^{-i\kappa\hat{\mathbf{x}}\cdot\mathbf{y}}}{4\pi} a(\mathbf{y}) \mathbf{E}(\mathbf{y}) \, \mathrm{d}\mathbf{y} - i\kappa\hat{\mathbf{x}} \int_{B_\rho} \frac{e^{-i\kappa\hat{\mathbf{x}}\cdot\mathbf{y}}}{4\pi} \frac{\mathbf{grad}\, a(\mathbf{y})}{1 - a(\mathbf{y})} \cdot \mathbf{E}(\mathbf{y}) \, \mathrm{d}\mathbf{y} \tag{5}$$

after a straightforward computation. Since the far field pattern is a tangential field, i.e. the orthogonal projection $\hat{\mathbf{x}} \times \mathbf{E}^\infty(\hat{\mathbf{x}}) \times \hat{\mathbf{x}}$ of $\mathbf{E}^\infty(\hat{\mathbf{x}})$ onto the tangent plane at $\hat{\mathbf{x}}$ coincides with $\mathbf{E}^\infty(\hat{\mathbf{x}})$, it follows that $\mathbf{E}^\infty = \mathbf{Z}(a\mathbf{E})$ with the far-field operator $\mathbf{Z} : L^2(B_\rho)^3 \to L^2(S^2)^3$ defined by

$$(\mathbf{Z}\mathbf{u})(\hat{\mathbf{x}}) := -\kappa^2 \hat{\mathbf{x}} \times \int_{B_\rho} \frac{e^{-i\kappa\hat{\mathbf{x}}\cdot\mathbf{y}}}{4\pi} \mathbf{u}(\mathbf{y}) \, \mathrm{d}\mathbf{y} \times \hat{\mathbf{x}}. \tag{6}$$

This formula was used in our computations to evaluate the far field pattern.

3 Discretization of the electromagnetic Lippmann-Schwinger equation

Concerning the numerical solution of the electromagnetic Lippmann-Schwinger equation (4), the main complication compared to the acoustic case are caused by the last term on the left hand side. This term is responsible for worse mapping properties of the integral operator, and it does not allow us to use $a\mathbf{E}$ as new unknown after multiplying the equation by a.

periodization. Let $\mathbf{f} : \mathbb{R}^3 \to \mathbb{C}^3$ and $k : \mathbb{R}^3 \to \mathbb{C}$ be the 4ρ-periodic functions in x_1, x_2, and x_3 defined by

$$\mathbf{f}(\mathbf{x}) := \chi(\mathbf{x})\mathbf{E}^i(\mathbf{x}), \qquad k(\mathbf{x}) := \begin{cases} \kappa^2 \Phi(\mathbf{x}), & |\mathbf{x}| < 2\rho, \\ 0, & |\mathbf{x}| \geq 2\rho, \end{cases}$$

for $\mathbf{x} \in G_{2\rho} := \{\mathbf{x} \in \mathbb{R}^3 : |x_j| < 2\rho, j = 1, 2, 3\}$. Here $\chi : \mathbb{R}^3 \to \mathbb{R}$ is a smooth cut-off function satisfying $\chi(\mathbf{x}) = 1$ for $|\mathbf{x}| \leq \rho$ and $\operatorname{supp}\chi \subset G_{2\rho}$, It is also possible to use smooth convolution kernels k, but in a three-dimensional setting this does not improve the mapping properties of the convolution operator, which are determined by the singularity of Φ. Therefore, we do not consider this possibility here. Furthermore, we introduce the function

$$\mathbf{b}(\mathbf{x}) := \frac{\operatorname{\mathbf{grad}} a(\mathbf{x})}{\kappa^2(1 - a(\mathbf{x}))}, \qquad \mathbf{x} \in \mathbb{R}^3.$$

Note that $\mathbf{b}(\mathbf{x})$ is well defined since $\operatorname{Re} n(\mathbf{x}) > 0$ for all $\mathbf{x}$. As $k(\mathbf{x}) = \kappa^2 \Phi(\mathbf{x})$ for $|\mathbf{x}| \leq 2\rho$, a function $\tilde{\mathbf{E}} \in L^2(B_\rho)^3$ satisfies

$$\tilde{\mathbf{E}}(\mathbf{x}) + \int_{B_\rho} k(\mathbf{x} - \mathbf{y})a(\mathbf{y})\tilde{\mathbf{E}}(\mathbf{y}) \, \mathrm{d}\mathbf{y} + \operatorname{\mathbf{grad}} \int_{B_\rho} k(\mathbf{x} - \mathbf{y})\mathbf{b}(\mathbf{y}) \cdot \tilde{\mathbf{E}}(\mathbf{y}) \, \mathrm{d}\mathbf{y} = \mathbf{f}(\mathbf{x})$$

for all $\mathbf{x} \in B_\rho$ if and only if it satisfies (4) for $\mathbf{x} \in B_\rho$. Given a solution $\tilde{\mathbf{E}}$ to the previous equation, a solution $\mathbf{E}$ to (4) can be computed by

$$\mathbf{E}(\mathbf{x}) := \mathbf{E}^i(\mathbf{x}) - \kappa^2 \int_{B_\rho} \Phi(\mathbf{x} - \mathbf{y})a(\mathbf{y})\tilde{\mathbf{E}}(\mathbf{y}) \, \mathrm{d}\mathbf{y} - \kappa^2 \operatorname{\mathbf{grad}} \int_{B_\rho} \Phi(\mathbf{x} - \mathbf{y})\mathbf{b}(\mathbf{y}) \cdot \tilde{\mathbf{E}}(\mathbf{y}) \, \mathrm{d}\mathbf{y}$$

for $\mathbf{x} \in \mathbb{R}^3$. Instead of $\mathbf{E}$ we will consider the multi-periodic function

$$\mathbf{u}(\mathbf{x}) := \mathbf{f}(\mathbf{x}) - \int_{B_\rho} k(\mathbf{x} - \mathbf{y})a(\mathbf{y})\tilde{\mathbf{E}}(\mathbf{y}) \, \mathrm{d}\mathbf{y} - \operatorname{\mathbf{grad}} \int_{B_\rho} k(\mathbf{x} - \mathbf{y})\mathbf{b}(\mathbf{y}) \cdot \tilde{\mathbf{E}}(\mathbf{y}) \, \mathrm{d}\mathbf{y},$$

$\mathbf{x} \in \mathbb{R}^3$ in the following. $\mathbf{u}$ satisfies the *periodic Lippmann-Schwinger equation*

$$\mathbf{u}(\mathbf{x}) + \int_{G_{2\rho}} k(\mathbf{x} - \mathbf{y})a(\mathbf{y})\mathbf{u}(\mathbf{y})\,\mathrm{d}\mathbf{y} + \mathbf{grad}\int_{G_{2\rho}} k(\mathbf{x} - \mathbf{y})\mathbf{b}(\mathbf{y}) \cdot \mathbf{u}(\mathbf{y})\,\mathrm{d}\mathbf{y} = \mathbf{f}(\mathbf{x})$$

for $\mathbf{x} \in G_{2\rho}$. With the convolution operator $K : L^2(G_{2\rho}) \to L^2(G_{2\rho})$,

$$(Kv)(\mathbf{x}) := \int_{G_{2\rho}} k(\mathbf{x} - \mathbf{y})v(\mathbf{y})\,\mathrm{d}\mathbf{y}, \qquad \mathbf{x} \in G_{2\rho}, \tag{7}$$

its component-wise application $\mathbf{K} : L^2(G_{2\rho})^3 \to L^2(G_{2\rho})^3$, and the abbreviations $\mathbf{Au} := \mathbf{K}(a\mathbf{u})$, $\mathbf{Bu} := \mathbf{grad}\,K(\mathbf{b} \cdot \mathbf{u})$, this equation can be written as

$$\mathbf{u} + \mathbf{Au} + \mathbf{Bu} = \mathbf{f}. \tag{8}$$

discretization. Let

$$\varphi_{\mathbf{j}}(\mathbf{x}) := (4\rho)^{-3/2}\exp\left(\frac{i\pi}{2\rho}\mathbf{j} \cdot \mathbf{x}\right), \qquad \mathbf{j} \in \mathbb{Z}^3, \mathbf{x} \in \mathbb{R}^3$$

denote the trigonometric orthonormal basis of $L^2(G_{2\rho})$ and let $\mathcal{T}_N := \mathrm{span}\,\{\varphi_{\mathbf{j}} : \mathbf{j} \in \mathbb{Z}_N^3\}$ where $\mathbb{Z}_N^3 := \{\mathbf{j} \in \mathbb{Z}^3 : -\frac{N}{2} \le j_1, j_2, j_3 < \frac{N}{2}\}$. The orthogonal projection of $L^2(G_{2\rho})$ onto $\mathcal{T}_N$ is given by

$$P_N v := \sum_{\mathbf{j} \in \mathbb{Z}_N^3} \hat{v}(\mathbf{j})\varphi_{\mathbf{j}}, \qquad \hat{v}(\mathbf{j}) := \int_{G_{2\rho}} v\overline{\varphi_{\mathbf{j}}}\,\mathrm{d}\mathbf{x}.$$

The trigonometric interpolation operator $Q_N : C(G_{2\rho}) \to \mathcal{T}_N$ maps a function $v \in C(G_{2\rho})$ to the unique trigonometric polynomial $Q_n v \in \mathcal{T}_N$ satisfying

$$(Q_N v)(h\mathbf{j}) = v(h\mathbf{j}) \qquad \text{for all } \mathbf{j} \in \mathbb{Z}_N^3$$

where $h = \frac{4\rho}{N}$. Moreover, we define $\mathbf{P}_N, \mathbf{Q}_N : L^2(G_{2\rho})^3 \to \mathcal{T}_n^3$ as the component-wise application of the operators P_N and Q_N, respectively.

Note that a complete system of eigenvectors and eigenvalues of the convolution operator K defined in (7) is given by

$$K\varphi_{\mathbf{j}} = (4\rho)^{3/2}\hat{k}(\mathbf{j})\varphi_{\mathbf{j}}, \qquad \mathbf{j} \in \mathbb{Z}^3. \tag{9}$$

We approximate the periodic Lippmann-Schwinger equation (8) by

$$\mathbf{u}_N + \mathbf{A}_N\mathbf{u}_N + \mathbf{B}_N\mathbf{u}_N = \mathbf{Q}_N\mathbf{f} \tag{10}$$

where

$$\mathbf{A}_N\mathbf{v} := \mathbf{K}\mathbf{Q}_N(a\mathbf{P}_N\mathbf{v}), \qquad \mathbf{B}_N\mathbf{v} := \mathbf{grad}\,KQ_N(\mathbf{b} \cdot \mathbf{P}_N\mathbf{v}).$$

Due to (9) any solution $\mathbf{u}_N$ to (10) belongs to $\mathcal{T}_N^3$. Therefore, we would obtain the same approximate solutions $\mathbf{u}_N$ if we replaced $\mathbf{P}_N$ by $\mathbf{I}$ in the definitions of $\mathbf{A}_N$ and $\mathbf{B}_N$. However, to analyze the computation of the adjoint as discussed in section 6, we need estimates of $\|\mathbf{A} - \mathbf{A}_N\| = \|(\mathbf{A} - \mathbf{A}_N)^*\|$ and $\|\mathbf{B} - \mathbf{B}_N\| = \|(\mathbf{B} - \mathbf{B}_N)^*\|$ (in norms to be specified below) with $\mathbf{A}_N$ and $\mathbf{B}_N$ as just defined. Moreover, the operator $\mathbf{P}_N$ in the definition of $\mathbf{A}_N$ and $\mathbf{B}_N$ will be needed in section 4 on multi-grid methods.

error analysis. For $\lambda \in \mathbb{R}$ let H^λ denote the periodic Sobolev space on $G_{2\rho}$ with the norm
$$\|v\|_\lambda := \Big(\sum_{\mathbf{j} \in \mathbb{Z}^3} (1 + |\mathbf{j}|^2)^\lambda |\hat{v}(\mathbf{j})|^2 \Big)^{1/2}$$
and $\mathbf{H}_\lambda := (H^\lambda)^3$ with norm $\|\mathbf{v}\|_\lambda := (\sum_{k=1}^3 \|v_k\|_\lambda^2)^{1/2}$. Here $|\mathbf{j}| := \sqrt{j_1^2 + j_2^2 + j_3^2}$ for $\mathbf{j} \in \mathbb{Z}^3$. The Fourier coefficients of the convolution kernel k have been computed in [1]: If $\pi|\mathbf{j}| \neq R$, $R := 2\rho\kappa$, then $(\hat{\underline{K}}_N)_0 = (4\rho)^{-3/2} \left(\mathrm{e}^{Ri}(1 - Ri) - 1 \right)$ and

$$(\hat{\underline{K}}_N)_{\mathbf{j}} = \frac{R^2(4\rho)^{-3/2}}{\pi^2|\mathbf{j}|^2 - R^2} \left\{ 1 - \mathrm{e}^{Ri} \left(\cos(\pi|\mathbf{j}|) - i\frac{R}{\pi|\mathbf{j}|} \sin(\pi|\mathbf{j}|) \right) \right\}, \quad \mathbf{j} \neq 0,$$

otherwise $(\hat{\underline{K}}_N)_{\mathbf{j}} = -i2^{-1/2} R(4\rho)^{-3/2}(1 - \mathrm{e}^{Ri} R^{-1} \sin(R))$. Since $|\hat{k}(\mathbf{j})| = \mathcal{O}(|\mathbf{j}|^{-2})$, we have $K \in L(H^\lambda, H^{\lambda+2})$ for all $\lambda \geq 0$ by virtue of (9). The identity

$$(\widehat{\mathbf{grad}\, v})(\mathbf{j}) = \frac{i\pi}{2\rho}\mathbf{j}\hat{v}(\mathbf{j}) \tag{11}$$

implies that $\mathbf{grad} \in L(H^{\lambda+1}, \mathbf{H}^\lambda)$ for all $\lambda \geq 0$. Finally, we need the estimate $\|vw\|_\lambda \leq c\|v\|_\lambda\|w\|_\lambda$, which holds for $\lambda > \frac{3}{2}$ with $c > 0$ independent of $v, w \in H^\lambda$ (cf. [1]). Let us assume that $n \in H^\mu$ with $\mu > \frac{5}{2}$. Putting everything together, we find that $\mathbf{A} \in L(\mathbf{H}^\lambda, \mathbf{H}^{\lambda+2})$ for $0 \leq \lambda \leq \mu$ and $\mathbf{B} \in L(\mathbf{H}^\lambda, \mathbf{H}^{\lambda+1})$ for $0 \leq \lambda \leq \mu - 1$. The compactness of the embedding $H^{\lambda_1} \hookrightarrow H^{\lambda_2}$ for $\lambda_1 > \lambda_2$ implies that $\mathbf{A}$ and $\mathbf{B}$ are compact in $L(\mathbf{H}^\lambda, \mathbf{H}^\lambda)$. Since uniqueness is inherited from (4), we obtain unique solvability of (8) in $\mathbf{H}^\lambda$, $0 \leq \lambda \leq \mu - 1$ for all right hand sides $\mathbf{f}$ using Riesz theory.

To analyze the approximation (10), we need the following estimates (cf. [12])

$$\|(Q_N - I)v\|_\lambda \leq cN^{\lambda-\mu}\|v\|_\mu, \qquad 0 \leq \lambda \leq \mu,\ \mu \geq 3/2, \tag{12}$$
$$\|(P_N - I)v\|_\lambda \leq cN^{\lambda-\mu}\|v\|_\mu, \qquad 0 \leq \lambda \leq \mu. \tag{13}$$

Here and in the following $c > 0$ denotes a generic constant whose value may change from line to line.

Lemma 1 *Let $n \in H^\mu$ with $\mu > \frac{5}{2}$ and $1 \leq \lambda \leq \mu$. Then there exists a constant $c > 0$ such that*

$$\|(\mathbf{A}_N + \mathbf{B}_N - \mathbf{A} - \mathbf{B})\mathbf{u}\|_\lambda \leq cN^{\lambda-\mu}\|\mathbf{u}\|_{\mu-1} \tag{14}$$

for all $\mathbf{u} \in \mathbf{H}^{\mu-1}$ and all $N \in \mathbb{N}$.

Proof. We will use the fact that for $v \in H^s$ and $w \in H^t$ with $s > 3/2$ and $t \in [0, s]$ we have $vw \in H^t$ and $\|vw\|_t \leq c\|v\|_s\|w\|_t$ (For $t = s$ see [1], and the case $t = 0$ follows from the continuity of the embedding $L^\infty \hookrightarrow H^s$. Now the statement for $t \in (0, s)$ can be obtained by interpolation.) Therefore, $a\mathbf{u} \in H^{\mu-1}$, and we get

$$
\begin{aligned}
\|\mathbf{A}_N\mathbf{u} - \mathbf{A}\mathbf{u}\|_\lambda &\leq \|\mathbf{K}\|_{\lambda\leftarrow\lambda-1}\|\mathbf{Q}_N(a\mathbf{P}_N\mathbf{u}) - a\mathbf{u}\|_{\lambda-1} \\
&\leq c\left(\|(\mathbf{Q}_N - \mathbf{I})(a\mathbf{P}_N\mathbf{u})\|_{\lambda-1} + \|a(\mathbf{P}_N - \mathbf{I})\mathbf{u}\|_{\lambda-1}\right) \\
&\leq c\left(N^{\lambda-\mu}\|a\mathbf{P}_N\mathbf{u}\|_{\mu-1} + \|a\|_{\mu-1} \cdot \|(\mathbf{P}_N - \mathbf{I})\mathbf{u}\|_{\lambda-1}\right) \leq cN^{\lambda-\mu}\|\mathbf{u}\|_{\mu-1}
\end{aligned}
$$

using (12) and (13). Moreover, we have $\mathbf{b} \in \mathbf{H}^{\mu-1}$ and $\mathbf{b} \cdot \mathbf{u} \in H^{\mu-1}$ under the given assumptions. Therefore, we obtain

$$
\begin{aligned}
\|\mathbf{B}_N\mathbf{u} - \mathbf{B}\mathbf{u}\|_\lambda &\leq \|\operatorname{grad} K\|_{\lambda\leftarrow\lambda-1}\|Q_N(\mathbf{b} \cdot \mathbf{P}_N\mathbf{u}) - \mathbf{b} \cdot \mathbf{u}\|_{\lambda-1} \\
&\leq c(\|(Q_N - I)(\mathbf{b} \cdot \mathbf{P}_N\mathbf{u})\|_{\lambda-1} + \|\mathbf{b} \cdot (\mathbf{P}_N - \mathbf{I})\mathbf{u}\|_{\lambda-1}) \\
&\leq cN^{\lambda-\mu}\|\mathbf{u}\|_{\mu-1}.
\end{aligned}
$$

as above. Combining these inequalities yields (14). $\square$

Theorem 2 *Let $\mu > \frac{5}{2}$, $1 \leq \lambda \leq \mu$, and assume that $n \in H^\mu$ and $\mathbf{f} \in \mathbf{H}^\mu$. Let $\mathbf{u} \in \mathbf{H}^{\mu-1}$ denote the unique solution to (8). Then there exist constants $N_0 \in \mathbb{N}$ and $c > 0$ such that (10) has a unique solution $\mathbf{u}_N$ for all $N \geq N_0$ and*

$$\|\mathbf{u}_N - \mathbf{u}\|_\lambda \leq cN^{\lambda-\mu}(\|\mathbf{u}\|_{\mu-1} + \|\mathbf{f}\|_\mu). \tag{15}$$

Proof. Since $\mathbf{I} + \mathbf{A} + \mathbf{B}$ is boundedly invertible in $\mathbf{H}^\lambda$, it follows from (14) by a Neumann series argument that $\mathbf{I} + \mathbf{A}_N + \mathbf{B}_N$ is boundedly invertible in $\mathbf{H}^\lambda$ for $N \geq N_0$ and that

$$\|(\mathbf{I} + \mathbf{A}_N + \mathbf{B}_N)^{-1}\|_{\lambda\leftarrow\lambda} \leq c \qquad \text{for all } N \geq N_0 \tag{16}$$

with a constant c independent of N. Therefore, (10) has a unique solution for $N \geq N_0$. Subtracting (8) from (10) yields the identity

$$(\mathbf{I} + \mathbf{A}_N + \mathbf{B}_N)(\mathbf{u}_N - \mathbf{u}) = \mathbf{Q}_N\mathbf{f} - \mathbf{f} + (\mathbf{A} + \mathbf{B} - \mathbf{A}_N - \mathbf{B}_N)\mathbf{u}.$$

Using (12), (14) and (16) we obtain

$$\|\mathbf{u}_N - \mathbf{u}\|_\lambda \leq c \left(\|(\mathbf{Q}_N - \mathbf{I})\mathbf{f}\|_\lambda + \|(\mathbf{A} + \mathbf{B} - \mathbf{A}_N - \mathbf{B}_N)\mathbf{u}\|_\lambda \right)$$
$$\leq cN^{\lambda-\mu}(\|\mathbf{f}\|_\mu + \|\mathbf{u}\|_{\mu-1}).$$

□

Since $f \in C^\infty$, Theorem 2 implies that the proposed discretization scheme converges of arbitrarily high order as $N \to \infty$ depending on the smoothness of the refractive index n. In particular, we have super-algebraic convergence for $n \in C^\infty$.

4   Solution of the discrete system

implementation of the operator $\mathbf{A}_N + \mathbf{B}_N$.   Next we discuss how the application of the operator $\mathbf{A}_N + \mathbf{B}_N$ can be implemented by FFT without the need to set up a matrix. For $w \in C(G_{2\rho})$ let $\underline{w}_N$ denote the vector of nodal values $w(h\mathbf{j})$, $\mathbf{j} \in \mathbb{Z}_N^3$, and $\underline{\hat{w}}_N$ the vector of the Fourier coefficients $\hat{w}(\mathbf{j})$ of w for $\mathbf{j} \in \mathbb{Z}_N^3$. The application of the matrix $F_N := \left(\exp(-\frac{2\pi i}{N}\mathbf{k} \cdot \mathbf{j}) \right)_{\mathbf{j},\mathbf{k}\in\mathbb{Z}_N^3}$ corresponds to the Fast Fourier Transform. We have $\underline{\hat{w}}_N = (4\rho)^{3/2}N^{-3}F_N\underline{w}_N$ and $\underline{w}_N = (4\rho)^{-3/2}F_N^*\underline{\hat{w}}_N$ for $w \in \mathcal{T}_N$.

It will be convenient to identify the vector $\underline{w}_N$ with the mapping $\mathbb{Z}_N^3 \to \mathbb{C}$ given by $\underline{w}_N(\mathbf{j}) = w(h\mathbf{j})$. For a vector valued function $\mathbf{w} \in C(G_{2\rho})^3$ we define $\underline{\mathbf{w}}_N, \hat{\mathbf{w}}_N : \mathbb{Z}_N^3 \to \mathbb{C}^3$ by $\underline{\mathbf{w}}_N(\mathbf{j}) := \mathbf{w}(h\mathbf{j})$ and $\hat{\mathbf{w}}_N(\mathbf{j}) := \hat{\mathbf{w}}(\mathbf{j})$, $\mathbf{j} \in \mathbb{Z}_N^3$. Again, $\mathbf{F}_N$ denotes the component-wise application of F_N.

For $\underline{v}, \underline{w} : \mathbb{Z}_N^3 \to \mathbb{C}$ and $\underline{\mathbf{v}}, \underline{\mathbf{w}} : \mathbb{Z}_N^3 \to \mathbb{C}^3$ we introduce the following binary operations:

$$(\underline{\mathbf{v}} \odot \underline{\mathbf{w}}) : \mathbb{Z}_N^3 \to \mathbb{C}, \qquad (\underline{\mathbf{v}} \odot \underline{\mathbf{w}})(\mathbf{j}) := \underline{\mathbf{v}}(\mathbf{j})^T\underline{\mathbf{w}}(\mathbf{j}),$$
$$(\underline{v} * \underline{w}) : \mathbb{Z}_N^3 \to \mathbb{C}, \qquad (\underline{v} * \underline{w})(\mathbf{j}) := \underline{v}(\mathbf{j})\underline{w}(\mathbf{j})$$
$$(\underline{v} * \underline{\mathbf{w}}), (\underline{\mathbf{w}} * \underline{v}) : \mathbb{Z}_N^3 \to \mathbb{C}^3, \qquad (\underline{v} * \underline{\mathbf{w}})(\mathbf{j}) := (\underline{\mathbf{w}} * \underline{v})(\mathbf{j}) := \underline{v}(\mathbf{j})\underline{\mathbf{w}}(\mathbf{j})$$

The gradient of a trigonometric polynomial $v \in \mathcal{T}_N$ is given by $(\mathbf{grad}\,v)_N = \mathbf{F}_N^*(\hat{\mathbf{g}} * F_N\underline{v}_N)$ where $\hat{\mathbf{g}} : \mathbb{Z}_N^3 \to \mathbb{C}^3$ is defined by $\hat{\mathbf{g}}(\mathbf{j}) := \frac{i\pi}{2\rho}\mathbf{j}$. Finally we use the relation $(\underline{K}\underline{w})_N = F_N^*\underline{\hat{K}}_N F_N\underline{w}_N$, $w \in \mathcal{T}_N$ with $\underline{\hat{K}}_N := (4\rho)^{3/2}N^{-3}\underline{\hat{k}}_N$, which follows from (9).

Using these notations and the fact the every solution to (10) belongs to $\mathcal{T}_N^3$, it follows that eq. (10) (an operator equation in $\mathbf{H}_\lambda$) is equivalent to the fully discrete system

$$\underline{\hat{\mathbf{u}}}_N + \underline{\hat{K}}_N * \mathbf{F}_N(\underline{a}_N * (\mathbf{F}_N^*\underline{\hat{\mathbf{u}}}_N)) + \hat{\mathbf{g}}_N * \underline{\hat{K}}_N * F_N(\underline{\mathbf{b}}_N \odot (\mathbf{F}_N^*\underline{\hat{\mathbf{u}}}_N)) = \widehat{(\mathbf{Q}_N\mathbf{f})}_N \quad (17)$$

which we shortly write as

$$\hat{\mathbf{u}}_N + \underline{\mathbf{T}}_N \hat{\mathbf{u}}_N = \widehat{(\mathbf{Q}_N \mathbf{f})}_N. \tag{18}$$

solution of the discrete system. Since the matrix $\underline{\mathbf{T}}_N$ in (18) is large and dense, it usually does not fit into the storage of a computer. Therefore (18) has to be solved by iterative method using (17) to implement matrix-vector products with $\underline{\mathbf{T}}_N$. One option is the conjugate gradient method applied to the normal equation (CGNE). Due to (16) the condition numbers of the operators $\mathbf{I} + \mathbf{T}_N$ are uniformly bounded by a constant γ

$$\|(\mathbf{I} + \mathbf{T}_N)^{-1}\|_{\lambda \leftarrow \lambda} \, \|\mathbf{I} + \mathbf{T}_N\|_{\lambda \leftarrow \lambda} \leq \gamma$$

for $N \geq N_0$ and $\lambda \geq 1$. Therefore, the error of the j-th CGNE-iterate $\mathbf{u}_N^{(j)}$ is bounded by

$$\|\mathbf{u}_N^{(j)} - \mathbf{u}_N\|_\lambda \leq c \left(\frac{\gamma - 1}{\gamma + 1} \right)^j \|\mathbf{u}_N^{(0)} - \mathbf{u}_N\|_\lambda \tag{19}$$

with a constant c independent of N (see, e.g. [13]). To be consistent with theory, we have to work in spaces $\mathbf{H}^\lambda$ with $\lambda \geq 1$. This corresponds to solving the preconditioned equation

$$\underline{\mathbf{\Lambda}}_\lambda (\mathbf{I}_N + \underline{\mathbf{T}}_N) \underline{\mathbf{\Lambda}}_\lambda^{-1} \hat{\mathbf{v}}_N = \underline{\mathbf{\Lambda}}_\lambda \widehat{(\mathbf{Q}_N \mathbf{f})}_N \tag{20}$$

for $\hat{\mathbf{v}}_N = \underline{\mathbf{\Lambda}}_\lambda \hat{\mathbf{u}}_N$ with $(\underline{\mathbf{\Lambda}}_\lambda \hat{\mathbf{u}}_N)(j) := (1 + |j|^2)^{\lambda/2} \hat{\mathbf{u}}_N(j)$, $j \in \mathbb{Z}_N^3$. Since we observed little differences in the results when replacing (18) by (20), we will work with (18) in the following for simplicity.

Another possibility is to solve eq. (18) by the GMRES method (see [13]). Although no convergence estimates are available in this case, GMRES was more efficient then CGNE in our numerical experiments, especially for large wave numbers.

multi-grid methods. A more efficient method to solve (18) is a two-grid iteration. We multiply (18) by the inverse $(\mathbf{I} + \mathbf{T}_M)^{-1}$ of the operator corresponding to a coarser discretization level $M < N$ and rewrite the resulting equation as a fixed-point equation:

$$\mathbf{u}_N^{(0)} := (\mathbf{I} + \mathbf{T}_M)^{-1} \mathbf{Q}_N \mathbf{f}, \tag{21a}$$

$$\mathbf{u}_N^{(j)} := (\mathbf{I} + \mathbf{T}_M)^{-1} \left\{ (\mathbf{T}_M - \mathbf{T}_N) \mathbf{u}_N^{(j-1)} + \mathbf{Q}_N \mathbf{f} \right\}, \quad j = 1, 2, \dots. \tag{21b}$$

To derive a fully discrete analog of (21b), recall that we interpret the vector $\hat{\mathbf{u}}_N \in \mathbb{C}^{3|\mathbb{Z}_N^3|}$ as a mapping $\hat{\mathbf{u}}_N : \mathbb{Z}_N^3 \to \mathbb{C}^3$ and that we introduced the matrix

$\underline{\mathbf{T}}_N \in \mathbb{C}^{3|\mathbb{Z}_N^3| \times 3|\mathbb{Z}_N^3|}$ in (18) via its action (18) on a vector $\hat{\underline{\mathbf{u}}}_N$. Let $\underline{\mathbf{R}}_{N,M} \in \mathbb{C}^{3|\mathbb{Z}_M^3| \times 3|\mathbb{Z}_N^3|}$ be the restriction matrix defined by $(\underline{\mathbf{R}}_{N,M}\hat{\underline{\mathbf{u}}}_N)(j) = \hat{\underline{\mathbf{u}}}_N(j)$ for $j \in \mathbb{Z}_M^3$. Its adjoint $\underline{\mathbf{R}}_{N,M}^* \in \mathbb{C}^{3|\mathbb{Z}_N^3| \times 3|\mathbb{Z}_M^3|}$ is the prolongation matrix given by

$$(\underline{\mathbf{R}}_{N,M}^*\hat{\underline{\mathbf{u}}}_M)(\mathbf{j}) = \begin{cases} \hat{\underline{\mathbf{u}}}_M(\mathbf{j}), & \mathbf{j} \in \mathbb{Z}_M^3, \\ 0, & \mathbf{j} \in \mathbb{Z}_N^3 \setminus \mathbb{Z}_M^3. \end{cases}$$

Moreover, we define the projection $\underline{\mathbf{P}}_{N,M} := \underline{\mathbf{I}}_N - \underline{\mathbf{R}}_{N,M}^*\underline{\mathbf{R}}_{N,M}$ onto the high frequency components in $\mathbb{C}^{3|\mathbb{Z}_N^3|}$. With these notations the matrix version of the two-grid iteration (21b) is

$$\hat{\underline{\mathbf{u}}}_N^{(j)} := \left(\underline{\mathbf{P}}_{N,M} + \underline{\mathbf{R}}_{N,M}^*(\underline{\mathbf{I}}_M + \underline{\mathbf{T}}_M)^{-1}\underline{\mathbf{R}}_{N,M} \right)$$
$$\times \left\{ (\underline{\mathbf{R}}_{N,M}^*\underline{\mathbf{T}}_M\underline{\mathbf{R}}_{N,M} - \underline{\mathbf{T}}_N)\hat{\underline{\mathbf{u}}}_N^{(j-1)} + \hat{\underline{\mathbf{f}}}_N \right\}.$$

To apply the operator $\mathbf{I} + \mathbf{T}_M$ (i.e. solve equations on the coarse grid) we can use CGNE or GMRES as described above. Since vectors on the coarse grid required much less storage, we usually do not run into memory problems with GMRES even though all previous iterates have to be stored.

Another idea, leading to multi-grid methods, is to approximate $(\mathbf{I} + \mathbf{T}_M)^{-1}$ by using a two-grid method on an even coarser grid. Let $N_1 < N_2 < \cdots < N_L$ be a sequence of discretization levels. For simplicity we restrict ourselves to a V-cycle scheme, i.e. we assume that just one iterations of the form (21b) is performed on each level. For a given right hand side $\mathbf{f}$ this leads to the following recursive definition of the multi-grid approximations $MG_l(\hat{\underline{\mathbf{v}}}, \hat{\underline{\mathbf{f}}}) \approx \hat{\underline{\mathbf{u}}}$ to the solution of $\hat{\underline{\mathbf{u}}} + \underline{\mathbf{T}}_{N_l}\hat{\underline{\mathbf{u}}} = \hat{\underline{\mathbf{f}}}_{N_l}$ given an initial guess $\hat{\underline{\mathbf{v}}} \in \mathbb{C}^{3|\mathbb{Z}_{N_l}^3|}$ and a right hand side $\hat{\underline{\mathbf{f}}} \in \mathbb{C}^{3|\mathbb{Z}_{N_l}^3|}$:

$$MG_l\left(\hat{\underline{\mathbf{v}}}, \hat{\underline{\mathbf{f}}}\right) := \underline{\mathbf{P}}_{N_l,N_{l-1}}\hat{\underline{\mathbf{w}}} + \underline{\mathbf{R}}_{N_l,N_{l-1}}^* MG_{l-1}\left(\underline{\mathbf{R}}_{N_l,N_{l-1}}\hat{\underline{\mathbf{v}}}, \underline{\mathbf{R}}_{N_l,N_{l-1}}\hat{\underline{\mathbf{w}}}\right)$$
$$\text{where } \hat{\underline{\mathbf{w}}} := \left(\underline{\mathbf{T}}_{N_{l-1}} - \underline{\mathbf{T}}_{N_l}\right)\hat{\underline{\mathbf{v}}} + \hat{\underline{\mathbf{f}}}_{N_l}$$

On the coarsest level $l = 1$ we solve the equation exactly,

$$MG_1\left(\hat{\underline{\mathbf{v}}}, \hat{\underline{\mathbf{f}}}\right) := (\underline{\mathbf{I}}_{N_1} + \underline{\mathbf{T}}_{N_1})^{-1}\hat{\underline{\mathbf{f}}}$$

(or by CGNE/GMRES with low tolerances in practice). A full multi-grid method for the solution of $(\underline{\mathbf{I}}_{N_L} - \underline{\mathbf{T}}_{N_L})\hat{\underline{\mathbf{u}}} = \hat{\underline{\mathbf{f}}}_{N_L}$ is then given by

$$\hat{\underline{\mathbf{v}}}_1^{(0)} := MG_l\left(\mathbf{0},\ \hat{\underline{\mathbf{f}}}_{N_1}\right),$$

$$\hat{\underline{\mathbf{v}}}_l^{(0)} := MG_l\left(\underline{\mathbf{P}}_{N_l,N_{l-1}}\hat{\underline{\mathbf{f}}}_{N_l} + \underline{\mathbf{R}}^*_{N_l,N_{l-1}}\hat{\underline{\mathbf{v}}}_{l-1}^{(0)},\ \hat{\underline{\mathbf{f}}}_{N_l}\right),\quad l = 2,\ldots,L,$$

$$\hat{\underline{\mathbf{v}}}_L^{(j)} := MG_L\left(\hat{\underline{\mathbf{v}}}_L^{(j-1)},\ \hat{\underline{\mathbf{f}}}_{N_L}\right),\qquad j = 1,2,\ldots$$

convergence analysis. Due to Lemma 1 and eq. (16) there exist constants $N_0, c > 0$ such that the iteration operators $\mathbf{T}_{M,N} := (\mathbf{I} - \mathbf{T}_M)^{-1}(\mathbf{T}_M - \mathbf{T}_N)$ are bounded by

$$\|\mathbf{T}_{M,N}\|_{\lambda\leftarrow\lambda} \le cM^{-1}$$

for $N_0 \le M \le N$. Moreover, using (12) and Theorem 2, the initial error is bounded by

$$\|\mathbf{u}_N^{(0)} - \mathbf{u}_N\| \le \|(\mathbf{I} + \mathbf{T}_M)^{-1}\|_{\lambda\leftarrow\lambda}\|(\mathbf{Q}_N - \mathbf{Q}_M)\mathbf{f}\|_\lambda + \|\mathbf{u}_M - \mathbf{u}\|_\lambda + \|\mathbf{u}_N - \mathbf{u}\|_\lambda$$
$$\le cM^{\lambda-\mu}(\|\mathbf{f}\|_\mu + \|\mathbf{u}\|_{\mu-1}).$$

Therefore, the convergence of the two-grid iteration can be estimated by

$$\|\mathbf{u}_N^{(j)} - \mathbf{u}_N\|_\lambda = \|\mathbf{T}_{M,N}^j(\mathbf{u}_N^{(0)} - \mathbf{u}_N)\|_\lambda \le \|\mathbf{T}_{M,N}\|^j\|\mathbf{u}_N^{(0)} - \mathbf{u}_N\|_\lambda$$
$$\le cM^{-j+\lambda-\mu}(\|\mathbf{f}\|_\mu + \|\mathbf{u}\|_{\mu-1}). \tag{22}$$

We want to choose the number J of multi-grid iteration such that (18) is solved at least up to an accuracy of the discretization error,

$$\|\mathbf{u}_N^{(J)} - \mathbf{u}_N\|_\lambda \le \epsilon\|\mathbf{u}_N - \mathbf{u}\|_\lambda \tag{23}$$

with some $\epsilon \in (0,1]$. If we choose

$$M \sim N^\theta \tag{24}$$

with a constant $\theta \in (0,1)$, then the estimates (15) and (22) of the discretization error and the two-grid convergence imply that (23) is achieved asymptotically if

$$\theta > \frac{\mu-1}{\mu-1+J}.$$

Using the convergence of the two-grid method, one can prove convergence of the multi-grid method in the standard way (see [14,15]). The multi-grid method converges if (24) is satisfied for any two subsequent levels with θ sufficiently large and if the coarsest grid is sufficiently fine.

complexity analysis. According to (18) the implementation of one matrix-vector product for the operator $\mathbf{I} + \mathbf{T}_N$ requires one backward vector FFT, one forward vector FFT and one forward scalar FFT. This makes a total of

7 scalar FFTs. Each FFT costs $O(N^3 \ln(N))$ arithmetical operations, and all other computations are of order $O(N^3)$.

It follows from (19) that the error $\|\mathbf{u}_N^{(j)} - \mathbf{u}_N\|$ of the CGNE iteration is comparable to the discretization error $cN^{\lambda-\mu}$ after at most $j \sim \ln N$ iterations. Since one iteration costs $O(N^3 \ln N)$ arithmetical operations, the total cost of the algorithm is
$$O(N^3 (\ln N)^2)$$
if the CGNE-iteration is used. For a two-grid method the same number $O(\ln N)$ of CGNE iterations is needed on the coarse grid. However, with the choice (24) the total cost for solving the coarse grid equation is of order $O(M^3 \ln M \ln N) = O(N^{3\theta} (\ln N)^2)$, which is negligable compared to one FFT on the fine grid. Hence, the total cost of a two-grid iteration is of order
$$O(N^3 \ln N).$$

For a multi-grid method satisfying (24) for any two subsequent levels, the total cost is also asymptotically dominated by the FFT operations on the finest grid. Therefore, in this asymptotic sense nothing is gained by introducing a multi-grid method. However, the above analysis does not keep track of the wave number. In our numerical experiments with high wave numbers we observed speed-up of up to 40% by introducing additional grids.

5   Numerical study of the forward solver

Tables 1 shows the convergence of our forward solver as the discretization level N tends to infinity. The computations were carried out on a 3 GHz Pentium IV machine with 2 GB RAM. The refractive index was
$$a(x_1, x_2, x_3) = -\exp\left(1 - \frac{1}{1 - (x_1^2 + (x_2 - 0.1)^2 + (x_3 + 0.1)^2)/0.81}\right) \quad (25)$$
for $x_1^2 + (x_2 - 0.1)^2 + (x_3 + 0.1)^2 \leq 0.81$ and $a(x) = 0$ else. The incident field was chosen as $E_i(x) = e^{ix_1} p$ with polarization $p^T = (0, 1, 0)$, and the measurement point was $\hat{\mathbf{x}}^T = (1, 0, 0)$. Fast convergence is clearly exhibited. For $N = 192$ we guess the number of correct digits by a comparison with $N = 180$. The iterations were stopped when the relative residual error was smaller than a tolerance of $5 \cdot 10^{-14}$. With this tolerance all digits shown in Table 1 agreed for CGNE and GMRES. As expected from (19), the number of CGNE/GMRES iterations is almost independent of the discretization level N. Our computer ran out of memory for $N = 192$ with CGNE and GMRES applied to eq. (18).

	CGNE/GMRES applied to (18)					two-grid method		
N	$\mathrm{Re}\,\mathbf{E}^\infty(\hat{\mathbf{x}})\cdot p$	CGNE #	time(s)	GMRES #	time(s)	$\mathrm{Re}\,\mathbf{E}^\infty(\hat{\mathbf{x}})\cdot p$	M	time(s)
24	**-0.0613**07198	27	0.8	9	0.4	**-0.0613**06584	8	0.1
48	**-0.06136**5886	27	6.9	9	3.5	**-0.06136**5836	16	0.8
96	**-0.061366**716	27	59.8	8	27.7	**-0.061366**708	24	7.1
192	-	-	-	-	-	**-0.06136666**3	36	81.4

Table 1

Convergence of the forward solver for $\kappa = 1$. The columns labeled with # contain the number of matrix-vector products with $\underline{\mathbf{T}}_N$ or $\underline{\mathbf{T}}_N^*$

	GMRES applied to (18)			two-grid method			
N	$\mathrm{Re}\,\mathbf{E}^\infty(\hat{\mathbf{x}})\cdot p$	GMRES(40) #	time(s)	$\mathrm{Re}\,\mathbf{E}^\infty(\hat{\mathbf{x}})\cdot p$	M	J	time(s)
48	**-0.75395587**	73	32.8	-	-	-	-
96	**-0.75475**045	74	276.9	**-0.75475**601	48	2	84.4
192	-	-	-	**-0.754755**85	48	4	216.2

Table 2

Convergence of the forward solver for $\kappa = 40$. The columns labeled with # contain the number of matrix-vector products with $\underline{\mathbf{T}}_N$ or $\underline{\mathbf{T}}_N^*$

For the two-grid method we performed $J = 2$ iteration and used GMRES on the coarse grid. M was chosen as an integer close to N^θ, $\theta = \frac{2}{3}$ with a prime factorization of the form $M = 2^n 3^m$. With these choices the error introduced by the two-grid iteration was always of the order of the discretization error. Moreover, the two-grid method is significantly faster and less memory intensive than CGNE and GMRES applied directly to (18).

Table 2 shows the convergence of our method for the wave number $\kappa = 40$. Here a finer coarse grid of at least $M = 48$ was necessary to represent the solution sufficiently accurately on the coarsest level. We used the inhomogeneity (25) shrinked by a factor 2 such that the diameter of the support was bounded by 1. We also observe fast convergence for this larger wave number.

Finally, in Table 3 we observed the dependence of the number of iterations on the wave number. It turns out that the number of CGNE iteration grows much faster than the number of GMRES iterations. Therefore, CGNE is not suited for large wave numbers. For GMRES we observe roughly a linear dependence of the number of iterations on the wave number.

κ	1	5	10	15	20	25	30	35	40	45	50
GMRES	8	12	23	34	47	55	62	68	74	80	90
CGNE	23	51	155	359				> 400			

Table 3

Dependence of the number of iterations on the wave number

6 The Fréchet derivative and its adjoint

For the solution of the inverse scattering problem we need to consider the operator

$$F : D(F) \subset H_0^s(B_\rho) \to L^2(S^2)^3, \qquad F(a) := \mathbf{E}^\infty$$

which maps a perturbation $a = 1 - n$ of the refractive index n to the corresponding far field pattern $\mathbf{E}^\infty$ of the scattered field. For simplicity, we first consider this operator for a fixed incident wave $\mathbf{E}^i$. Since we need a Hilbert space setting for the algorithms to be discussed below, we chose the domain of definition $D(F)$ of F to be the set of all functions a in the Sobolev space $H^s(B_\rho)$ with $a < 1$. Moreover, we let $s > \frac{5}{2}$ such that $H_0^s(B_\rho) \subset C_0^{1,\alpha}(B_\rho)$ for $0 < \alpha < \frac{5}{2}$. With the notations introduced above we can write down F in closed form:

$$F(a) = \mathbf{Z} a \Big(\mathbf{I} + \mathbf{K} a \bullet + \mathbf{grad}\, K \mathbf{b} \cdot \bullet \Big)^{-1} (\chi \mathbf{E}^i)$$

Using this formula it is a simple task to show that the operator F is Fréchet differentiable (see, e.g., [2, Prop. 2.1] for a similar argument). To obtain a formula for the Fréchet derivative $F'[a]h$, we differentiate the periodic Lippmann-Schwinger equation (8) with respect to a. This yields the following formula for the Fréchet derivative $\mathbf{u}'_{a,h}$ at a in the direction h of the periodic version $\mathbf{u} = \mathbf{u}_a$ of electric field $\mathbf{E}$

$$\mathbf{u}'_{a,h} + \mathbf{K}(a\mathbf{u}'_{a,h}) + \mathbf{grad}\, K \left(\frac{\mathbf{grad}\, a}{\kappa^2(1-a)} \cdot \mathbf{u}_{a,h} \right) = \mathbf{R}_a h$$

where the right hand side is given by

$$\mathbf{R}_a h = -\mathbf{K}(h\mathbf{u}_a) - \mathbf{grad}\, K \left(\frac{1}{\kappa^2} \left\{ \mathbf{grad}\, h + h \frac{\mathbf{grad}\, a}{1-a} \right\} \cdot \frac{\mathbf{u}_a}{1-a} \right).$$

Hence, we can compute $\mathbf{u}'_{a,h}$ by solving the periodic Lippmann-Schwinger equation (8) with a different right hand side. The derivative of F is given by

$$F'[a]h = \mathbf{Z} \left(a\mathbf{u}'_{a,h} + h\mathbf{u}_a \right).$$

15

The adjoint of the operator $F'[a]$ with respect to the L^2-norm is given by

$$F'[a]_{L^2}^* \mathbf{g} = \overline{\mathbf{u}_a} \cdot \mathbf{Z}^* \mathbf{g} + \mathbf{R}_{a,L^2}^* \left(\mathbf{I} + \overline{a} \mathbf{K}^* \bullet - \overline{\mathbf{b}} K^* \operatorname{div} \bullet \right)^{-1} \overline{a} \mathbf{Z}^* \mathbf{g}$$

with the adjoint operators

$$(\mathbf{Z}^* \mathbf{g})(\mathbf{y}) = -\kappa^2 \int_{S^2} e^{i\kappa \mathbf{y} \cdot \hat{\mathbf{x}}} (\hat{\mathbf{x}} \times \mathbf{g}(\hat{\mathbf{x}}) \times \hat{\mathbf{x}}) \, ds(\hat{\mathbf{x}})$$

and

$$\mathbf{R}_{a,L^2}^* \mathbf{u} = -\overline{\mathbf{u}_a} \cdot \mathbf{K}^* \mathbf{u} + \frac{1}{\kappa^2} \left\{ -\operatorname{div} + \frac{(\mathbf{grad}\, \overline{a})}{1 - \overline{a}} \right\} \frac{\overline{\mathbf{u}_a}}{1 - \overline{a}} K^* \operatorname{div} \mathbf{u}.$$

Obviously, the operator $\mathbf{I} + \mathbf{A}^* + \mathbf{B}^*$ in (8) can be approximated by $\mathbf{I} + \mathbf{A}_N^* + \mathbf{B}_N^*$, and the error estimate (14) is also valid for the adjoint operators. (Again all adjoints are with respect to the L^2-inner product.) It is important for the stability of the inverse solver to use the adjoint $F'[a]^*$ of $F'[a]$ with respect to the H^s-norm instead of the L^2-adjoint $F'[a]_{L^2}^*$. If $j : H^s(B_\rho) \hookrightarrow L^2(B_\rho)$ is the embedding operator, these two adjoint operators are related by

$$F'[a]^* = j^* F'[a]_{L^2}^*.$$

An efficient method to implement j^* for Sobolev indices $s \in \mathbb{N}$ has been described in [2] using the Gram matrix for a basis of tensor products of splines and spherical harmonics.

Remark. If a is small, then $\mathbf{u}_a \approx \chi \mathbf{E}^i$, and the scattered field $\mathbf{u}_a - \chi \mathbf{E}^i$ is small compared to $\mathbf{u}_a$. Since $\chi \mathbf{E}^i$ does not depend on a, $\mathbf{u}_{a,h}'$ is typically small compared to $\mathbf{u}_a$ as well. Hence, we can use the approximation $F'[a]h \approx \mathbf{Z}(h\mathbf{u}_a)$, which is much cheaper to compute since it avoids solving another operator equation. It is an improvement of the Born approximation $F'[a]h \approx \mathbf{Z}(h\chi \mathbf{E}^i)$. However, both approximations break down if a or κ are medium or large. In particular, we could not use this approximation in the examples reported below.

7   The inverse problem

We now consider the problem to recover the refractive index of a medium from measurements of far field patterns of scattered electric waves. Since the far-field pattern $\mathbf{E}^\infty$ for one incident field is a function of 2 variables whereas the unknown refractive index is a function of 3 variables, we have to use many incident fields. Consider incident fields of the form

$$\mathbf{E}^i(\mathbf{x}) = \mathbf{p} e^{-i\kappa \mathbf{x} \cdot \mathbf{d}}$$

with direction $\mathbf{d} \in \mathbb{R}^3$, $|\mathbf{d}| = 1$ and polarization $\mathbf{p} \in \mathbb{C}^3$ such that $\mathbf{p} \cdot \mathbf{d} = 0$. The corresponding far-field patterns are denoted by $\mathbf{E}^\infty(\hat{\mathbf{x}}, \mathbf{d}; \mathbf{p})$. Due to the linearity of the partial differential equation, the dependence of the far-field pattern $\mathbf{E}^\infty$ on the polarization $\mathbf{p}$ is linear, so we can write

$$\mathbf{E}^\infty(\hat{\mathbf{x}}, \mathbf{d}; \mathbf{p}) = \mathbf{e}^\infty(\hat{\mathbf{x}}, \mathbf{d})\mathbf{p}$$

with a matrix $\mathbf{e}^\infty(\hat{\mathbf{x}}, \mathbf{d}) \in \mathbb{C}^{3 \times 3}$. With the convention $\mathbf{e}^\infty(\hat{\mathbf{x}}, \mathbf{d})\mathbf{d} = 0$, the matrix $\mathbf{e}^\infty(\hat{\mathbf{x}}, \mathbf{d})$ is uniquely determined. Since $\hat{\mathbf{x}} \cdot \mathbf{e}^\infty(\hat{\mathbf{x}}, \mathbf{d})\mathbf{p} = \hat{\mathbf{x}} \cdot \mathbf{E}^\infty(\hat{\mathbf{x}}, \mathbf{d}; \mathbf{p}) = 0$ for all $\mathbf{p}$, $\mathbf{e}^\infty(\hat{\mathbf{x}}, \mathbf{d})$ can be described by only 4 complex numbers.

With this notation we can formulate the inverse problem as an operator equation

$$F(a) = \mathbf{e}^\infty \tag{26}$$

with the operator

$$F : D(F) \subset H_0^s(B_\rho) \to L^2(S^2 \times S^2, \mathbb{C}^{3 \times 3}), \qquad s > \frac{5}{2}$$

which maps a perturbation $a(\mathbf{x})$ of the refractive index $n(\mathbf{x})$ to the far field matrix $\mathbf{e}^\infty(\hat{\mathbf{x}}, \mathbf{d})$ for all directions $\hat{\mathbf{x}} \in S^2$ of the incident field and all measurement directions $\mathbf{d} \in S^2$. It is straightforward to accommodate for partial data in this formalism. It is known that the operator F is one-to-one (see Colton & Päivärinta [16]), i.e. the refractive index is uniquely determined by the far field patterns of all incident plane waves.

In practice only noisy data $\mathbf{e}_\delta^\infty$ will be available. To be able to construct a convergent regularization method we need to know a bound δ on the noise level (see [17, Theo. 3.3]):

$$\|\mathbf{e}_\delta^\infty - \mathbf{e}^\infty\|_{L^2} \le \delta$$

Preconditioned Newton method. The iteratively regularized Gauss-Newton method [17] for the solution of (26) consists in applying Tikhonov regularization with initial guess a_0 to the Newton equation $F'[a_n](a_{n+1} - a_n) = \mathbf{e}_\delta^\infty - F(a_n)$. Hence, the regularized Newton iterates are computed by solving the quadratic minimization problems

$$a_{n+1} = \mathrm{argmin}_{a \in H_0^s(B_\rho)}\|F'[a_n](a - a_n) - \mathbf{e}_\delta^\infty + F(a_n)\|^2 + \alpha_n\|a - a_0\|^2. \tag{27}$$

For local convergence results of this method we refer to [18,19]. We have always chosen the regularization parameters of the form $\alpha_n = \left(\frac{2}{3}\right)^n \alpha_0$. This simple rule yielded good results in all our examples. To globalize the convergence of the method, other choices of the regularization parameter and step size control methods may be useful (see [20]).

To avoid the computation of a matrix for the Fréchet derivative $F'[a_n]$, we solve the minimization problems (27) iteratively by the conjugate gradient method. This requires only the applications of the operators $F'[a_n]$ and $F'[a_n]^*$ to given vectors as described in section 6. Since $\alpha_n \to 0$ as $n \to \infty$, the condition number of the system (27) gets very large, so many CG-steps are required. The number of CG-steps can be significantly reduced by using a preconditioner. As explained in [2], a suitable preconditioner can be constructed by exploiting the close connection between the CG and the Lanczos method to compute approximations to the largest eigenvalues and -vectors of $F'[a_n]^* F'[a_n]$. This method has been used in our computations.

numerical results. We have tested our method for the refractive index given by

$$n(x_1, x_2, x_3) = 1 - \frac{0.25 \sin(5(x_1 - 1)x_3 + x_2(x_2 - 2))}{1.2 - \cos(x_1(x_1 - 2) + (x_3 - 0.5)x_3(x_3 + 1) + x_2)} \times$$
$$\times \chi(-0.8(1.5x_1 + x_2 + x_3 - 0.5))\chi(2.5(|x|_2 - 0.55))$$

with the cut-off function $\chi(t) := \sum_{j=-\infty}^{0} \chi_0(t - j) / \left(\sum_{j=-\infty}^{\infty} \chi_0(t - j)\right)$ and $\chi_0(t) := \exp(-1/(1 - t^2))$, $|t| < 1$, $\chi_0(t) := 0$ else (see Figures 1 – 3). The wave number was $\kappa = 5$. In Fig. 1 and 2 we used 80 incident waves from 40 different direction of an angle of $\leq \pi/3$ to the positive z−axis. The corresponding far-field patterns were evaluated in the same 40 directions, yielding a data set of 80×80 complex numbers. In two experiments we added 1% and 10% white noise to these synthetic data and stopped the Newton iterations using the discrepancy principle after 19 and 14 iterations, respectively. The Newton iterations were started at $a_0 \equiv 0$ with regularization parameter $\alpha_0 = 1$. The discretization level for the electric field was $N = 32$, whereas the refractive index was represented by 2496 unknowns using tensor products of spherical harmonics of order ≤ 12 and splines of degree for 4 with 30 knots in radial direction (see [2]). We have chosen the Sobolev index $s = 3$ to meet the requirement $s > \frac{5}{2}$. The computations were carried out on a 3 GHz Pentium IV machine with 2GB RAM and took about 5 hours for the noise level of 1%. Thanks to the use of the preconditioner the average number of CGNE iteration per Newton step was only 3.95. With the rather high noise level of 10% we could still recover the main features of the scatterer, but the reconstruction was smoothed out and details got lost. With 1% even some finer details such as the little valley in the lowest row of Fig 1 could be reconstructed correctly.

In a third experiment we tested the convergence of our iteration scheme on a data set with a very small noise level of $\delta = 10^{-4}$. Here we used 100 plane incident waves from 50 direction and 50 measurement points for the far field points with full aperture. To guarantee sufficient accuracy of our forward solver, the
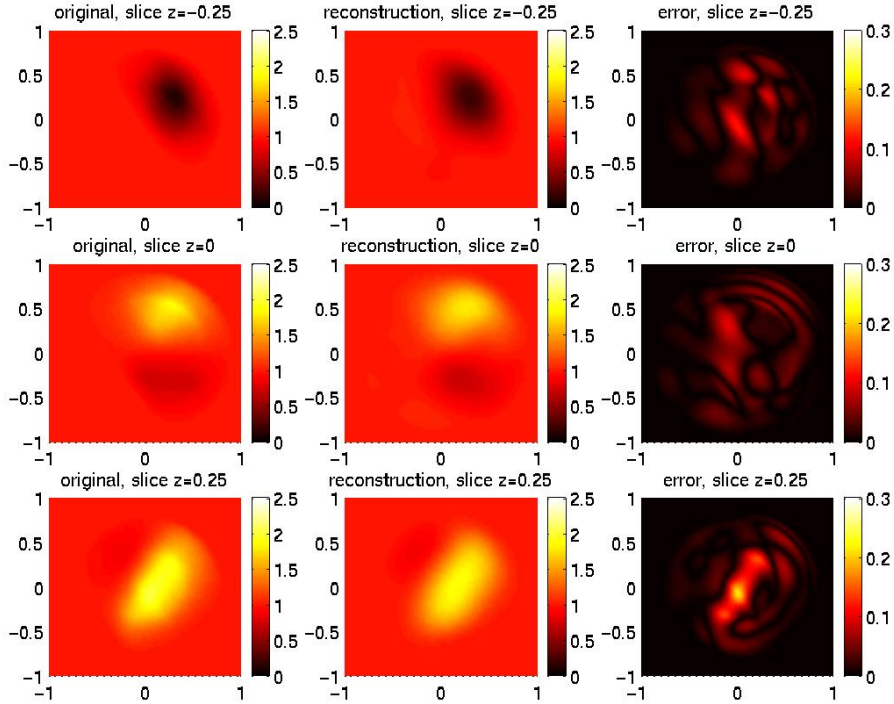
18

Fig. 1. Reconstruction with relative noise level $\delta = 10^{-2}$ and limited aperture

discretization level was chosen as $N = 96$ corresponding to 2.654.208 complex unknowns for the electric field for each incident wave. For the refractive index we used the same approximating subspace as above with the much smaller dimension 2496. This is sufficient as the best L^2-approximation to the true refractive index in that subspace was much more accurate than our reconstructions. The computations were carried out in parallel on a cluster of 12 Linux PCs. Since the computational cost of the preconditioned Newton iteration is largely dominated by the evaluations of F, $F'[a_n]h$ and $F'[a_n]^*g$ and since the forward solutions for different waves can be carried out in parallel by different processors, the parallel speed-up is almost proportional to the number of processors as long as the number of waves is much larger than the number of processors. Also for this small value of δ it was possible to reduce the residual $\|F(a_n) - \mathbf{e}_\delta^\infty\|$ to the order of the noise level, but the computations took about 4 days. The reconstruction of the refractive index shown in Fig. 3 is only about a factor 2 better than the reconstruction with $\delta = 10^{-2}$ in Fig. 1. This drastically illustrates the severe ill-posedness of the problem.
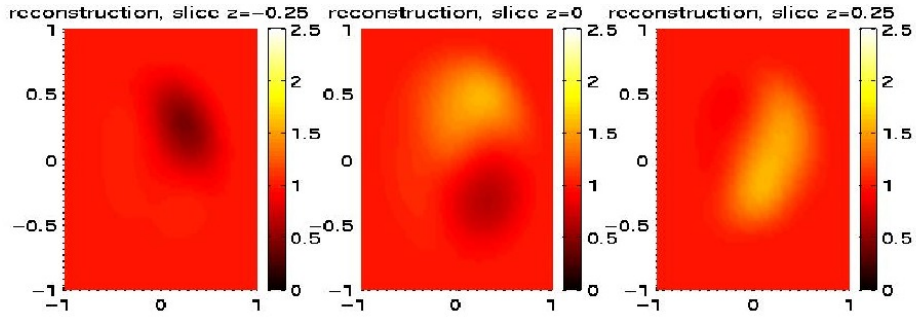
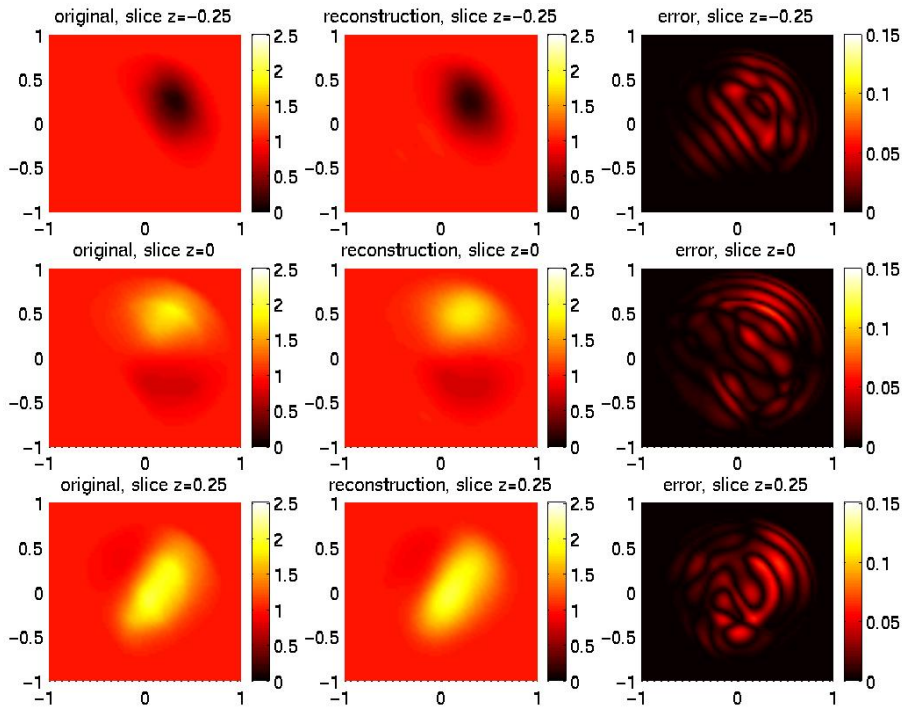Fig. 2. Reconstruction with relative noise level $\delta = 10^{-1}$ and limited aperture

Fig. 3. Reconstruction with relative noise level $\delta = 10^{-4}$ and full aperture

Acknowledgment

References

[1] G. M. Vainikko, Fast solvers of the Lippmann-Schwinger equation, in: R. P. Gilbert, J. Kajiwara, Y. S. Xu (Eds.), Direct and Inverse Problems of Mathematical Physics, Kluwer Acad. Publ., Dordrecht, 1999.

[2] T. Hohage, On the numerical solution of a three-dimensional inverse medium scattering problem, Inverse Problems 17 (2001) 1743–1763.

[3] F. Natterer, F. Wübbeling, A propagation - backpropagation method for ultrasound tomography, Inverse Problems 11 (1995) 1225–1232.

[4] M. Vögeler, Reconstruction of the three-dimensional refractive index in electromagnetic scattering using a propagation-backpropagation method, Inverse Problems 19 (2003) 739–753.

[5] G. Bao, P. Li, Inverse medium scattering for three-dimensional time harmonic Maxwell equations, Inverse Problems 20 (2004) L1–L7.

[6] Y. Chen, Inverse scattering via Heisenberg's uncertainity principle, Inverse Problems 13 (2001) 253–282.

[7] H. Haddar, P. Monk, The linear sampling method for solving the electromagnetic inverse medium problem, Inverse Problems 18 (2002) 891–906.

[8] A. Kirsch, The factorization method for Maxwell's equations, Inverse Problems 20 (2004) 117–134.

[9] K. J. Langenberg, Linear scalar inverse scattering, in: E. R. Pike, P. C. Sabatier (Eds.), Scattering: Scattering and Inverse Scattering in Pure and Applied Sciences, Academic, London, 2001, pp. 121–141.

[10] P. M. van den Berg, Non-linear scalar inverse scattering algorithms and applications, in: E. R. Pike, P. C. Sabatier (Eds.), Scattering: Scattering and Inverse Scattering in Pure and Applied Sciences, Academic, London, 2001, pp. 142–161.

[11] D. Colton, R. Kreß, Inverse Acoustic and Electromagnetic Scattering Theory, 2nd Edition, Springer Verlag, Berlin, Heidelberg, New York, 1997.

[12] S. Prössdorf, B. Silbermann, Numerical Analysis for Integral and Related Operator Equations, Birkhäuser, Basel, 1991.

[13] A. Greenbaum, Iterative Methods for Solving Linear Systems, SIAM, Philadelphia, 1997.

[14] W. Hackbusch, Multi-Grid Methods and Applications, Springer, Berlin, Heidelberg, New York, 1985.

[15] R. Kreß, Linear Integral Equations, 2nd Edition, Springer Verlag, Berlin, Heidelberg, New York, 1999.

[16] D. Colton, L. Päivärinta, The uniqueness of a solution to an inverse scattering problem for electromagnetic waves, Arch. Ration. Mech. Anal. 119 (1992) 59–70.

[17] H. W. Engl, M. Hanke, A. Neubauer, Regularization of Inverse Problems, Kluwer Academic Publisher, Dordrecht, Boston, London, 1996.

[18] B. Blaschke, A. Neubauer, O. Scherzer, On convergence rates for the iteratively regularized Gauß-Newton method, IMA Journal of Numerical Analysis 17 (1997) 421–436.

[19] T. Hohage, Logarithmic convergence rates of the iteratively regularized Gauß-Newton method for an inverse potential and an inverse scattering problem, Inverse Problems 13 (1997) 1279–1299.

[20] P. Deuflhard, Newton Methods for Nonlinear Problems. Affine Invariance and Adaptive Algorithms, Springer, Berlin, Heidelberg, 2004.

Institut für Numerische und Angewandte Mathematik

Universitt Göttingen

Lotzestr. 16-18

D - 37083 Göttingen

Telefon:	0551/394512
Telefax:	0551/393944

Email: trapp@math.uni-goettingen.de   URL: http://www.num.math.uni-goettingen.de

Verzeichnis der erschienenen Preprints:

2005-01	A. Schöbel, S. Scholl:	Line Planning with Minimal Traveling Time
2005-02	A. Schöbel	Integer programming approaches for solving the delay management problem
2005-03	A. Schöbel	Set covering problems with consecutive ones property
2005-04	S. Mecke, A. Schöbel, D. Wagner	Station location - Complex issues
2005-05	R. Schaback	Convergence Analysis of Methods for Solving General Equations
2005-06	M. Bozzini, L. Lenarduzzi, R. Schaback	Kernel B–Splines and Interpolation
2005-07	R. Schaback	Convergence of Unsymmetric Kernel–Based Meshless Collocation Methods
2005-08	T. Hohage, F.J. Sayas	Numerical solution of a heat diffusion problem by boundary element methods using the Laplace transform
2005-09	T. Hohage	An iterative method for inverse medium scattering problems based on factorization of the far field operator

2005-10	F. Bauer, T. Hohage	A Lepskij-type stopping rule for regularized Newton methods
2005-11	V. Dolean, F. Nataf, G. Rapin	New constructions of domain decomposition methods for systems of PDEs
		Nouvelles constructions de méthodes de décomposition de domaine pour des systèmes d'équations aux dérivées partielles
2005-12	F. Nataf, G. Rapin	Construction of a New Domain Decomposition Method for the Stokes Equations
2005-13	Y.C. Hon, R. Schaback	Solvability of Partial Differential Equations by Meshless Kernel Methods
2005-14	F. Bauer, P. Mathé, S. Pereverzev	Local Solutions to Inverse Problems in Geodesy: The Impact of the Noise Covariance Structure upon the Accuracy of Estimation
2005-15	O. Ivanyshyn, R. Kress	Nonlinear integral equations for solving inverse boundary value problems for inclusions and cracks
2005-16	R. Kress, W. Rundell	Nonlinear integral equations and the iterative solution for an inverse boundary value problem
2005-17	A. Yapar, H. Sahintürk, I. Akduman, R. Kress	One-Dimensional Profile Inversion of a Cylindrical Layer with Inhomogeneous Impedance Boundary: A Newton-Type Iterative Solution
2005-18	J. Puerto, A. Schöbel, S. Schwarze	The Path Player Game: Introduction and Equilibri
2005-19	R. Ahrens, A. Beckert, H. Wendland	A meshless spatial coupling scheme for large-scale fluid-structure-interaction problems
2005-20	F.J. Narcowich, J.D. Ward, X. Sun, H. Wendland	Direct and Inverse Sobolev Error Estimates for Scattered Data Interpolation via Spherical Basis Functions
2005-21	F.J. Narcowich, J.D. Ward, H. Wendland	Sobolev Error Estimates and a Bernstein Inequality for Scattered Data Interpolation via Radial Basis Functions
2005-22	I. Akduman, R. Kress, A. Yapar	Iterative Reconstruction of Dielectric Rough Surface Profiles at Fixed Frequency

2005-23	A. Schöbel, S. Scholl et.al.	DisKon - Disposition und Konfliktlsungsmanagement fr die beste Bahn
2005-24	P. Ivanyshyn, R. Kress	Nonlinear Integral Equations in Inverse Obstacle Scattering
2005-25	R. Kress, P. Serranho	A hybrid method for two-dimensional crack reconstruction
2005-26	R. Kress, P. Serranho	A hybrid method for sound-hard obstacle reconstruction
2005-27	G. Lube, G. Rapin	Residual-based stabilized higher-order FEM for advection-diffusion problems
2005-28	G. Lube, G. Rapin	Residual-based stabilized higher-order FEM for a generalized Oseen problem
2005-29	G. Lube, T. Knopp et.al.	Domain decomposition methods for indoor air flow simulation
2005-30	G. Lube et. al.	Stabilized finite element methods for the generalized Oseen problem
2005-31	R. Schaback	Multivariate interpolation by polynomials and radial basis functions
2005-32	R. Schaback	Inverse and Stability Estimates for Meshless Approximations by Translates of Kernel Functions
2005-33	R. Schaback	Kernel Techniques: From Machine Learning to Meshless Methods
2005-34	T. Hohage	Fast numerical solution of the electromagnetic medium scattering problem and applications to the inverse problem